Balmer-alpha and Balmer-beta Stark line intensity profiles for high-power hydrogen inductively coupled plasmas

2014 Chinese Phys. B 23 075201

(http://iopscience.iop.org/1674-1056/23/7/075201)

Balmer-alpha and Balmer-beta Stark line intensity profiles for high-power hydrogen inductively coupled plasmas*

Wang Song-Bai(王松柏)[a)b)], Lei Guang-Jiu(雷光玖)[c)†], Liu Dong-Ping(刘东平)[a)‡], and Yang Si-Ze(杨思泽)[a)]

[a)] School of Physics and Mechanical & Electrical Engineering, Xiamen University, Xiamen 361005, China
[b)] College of Physics and Information Engineering, Fuzhou University, Fuzhou 350108, China
[c)] Southwestern Institute of Physics, Chengdu 610041, China

(Received 12 October 2013; revised manuscript received 17 March 2014; published online 22 May 2014)

We compare Balmer-alpha (H_α) and Balmer-beta (H_β) emissions from high-power (1.0–6.0 kW) hydrogen inductively coupled plasmas (ICPs), and propose region I (0.0–2.0 kW), region II (2.0–5.0 kW), and region III (5.0–6.0 kW). In region I, both H_α emission intensity (I_α) and H_β emission intensity (I_β) increase with radio frequency (RF) power, which is explained by the corona model and Boltzmann's law, etc. However, in region II, I_α almost remains constant while I_β rapidly achieves its maximum value. In region III, I_α slightly increases with RF power, while I_β decreases with RF power, which deviates significantly from the theoretical explanation for the H_α and H_β emissions in region I. It is suggested that two strong electric fields are generated in high-power (2.0–6.0 kW) hydrogen ICPs: one is due to the external electric field of high-power RF discharge, and the other one is due to the micro electric field of the ions and electrons around the exited state hydrogen atoms in ICPs. Therefore, the strong Stark effect can play an important role in explaining the experimental results.

Keywords: high-power radio frequency plasma, H_α and H_β spectral lines in hydrogen ICPs, Stark effect

PACS: 52.27.Gr, 52.27.–h **DOI:** 10.1088/1674-1056/23/7/075201

1. Introduction

Neutral beam injection (NBI) can be generated by high-power radio frequency (RF) ion sources, which is one of the major plasma heating methods and plays an important role in the operation of large- and medium-sized Tokamaks, such as TFTR, JET, JT60, DIII-D, etc.[1] Since neutral atoms are not bound by the magnetic field, the atoms can freely move across the magnetic field and collide with other particles in the plasma. Analysis of the spectral lines emitted from hydrogen atoms at the high energy levels can provide some valuable information about the high-density RF plasma. As a non-invasive and powerful spectral diagnostic method, the optical emission spectroscopy (OES) has been rapidly developed and widely used for measuring the density and temperature of magnetically confined plasma.[2–5] Furthermore, the theoretical models for hydrogen excitation and ionization were presented by Johnson *et al.*[6] and Drawin *et al.*[7] Some software packages have been developed to simulate the hydrogen emission spectra.[8–12] However, most experimental results were obtained only from the low-density hydrogen plasmas generated in the RF discharge power range of < 200 W.[13–15] For high-density hydrogen plasmas in the RF power of > 1.0 kW, insufficient results were obtained due to the strong electromagnetic disturbance and technical processing difficulties.

In general, both Balmer-alpha (H_α) spectral line intensity (I_α) and Balmer-beta (H_β) spectral line intensity (I_β) increase with the input RF power.[13–15] Our experimental results showed that for the low-power (<1.0 kW) hydrogen inductively coupled plasmas (ICPs), both I_α and I_β increase with the RF power. However, it was found that both I_α and I_β do not increase with the input RF power in the range of 2.0–6.0 kW. Due to the strong electric field in high-power hydrogen ICPs, the strong Stark effect can be the main reason for the above experimental results.

In this paper, we illustrate the experiment phenomenon, and conduct the comparison and analysis of the experimental results. Finally, the physical explanation is given in detail.

2. Experimental apparatus

The experimental setup for generating high-power ICPs and the plasma diagnosis systems is schematically illustrated in Fig. 1. The ICPs discharge system was mainly composed of the RF ion source, the matching network, the quartz tube, and the electrode coil. The frequency of the RF ion source was 2 MHz and its output power can be adjustable in the range from 0.0 to 6.0 kW. The quartz tube was 180 mm long and 260 mm in diameter. The electrode coil was made of four turns of water-cooled copper coils. The vacuum system included a mechanical (15 L/s) and a molecular pump (1600 L/s). The background vacuum of the discharge chamber

*Project supported by the National Magnetic Confinement Fusion Science Program of China (Grant Nos. 2011GB108011 and 2010GB103001) and the Major International (Regional) Project Cooperation and Exchanges (Grant No. 11320101005).

†Corresponding author. E-mail: gjlei@swip.ac.cn
‡Corresponding author. E-mail: dongping.liu@dlnu.edu.cn

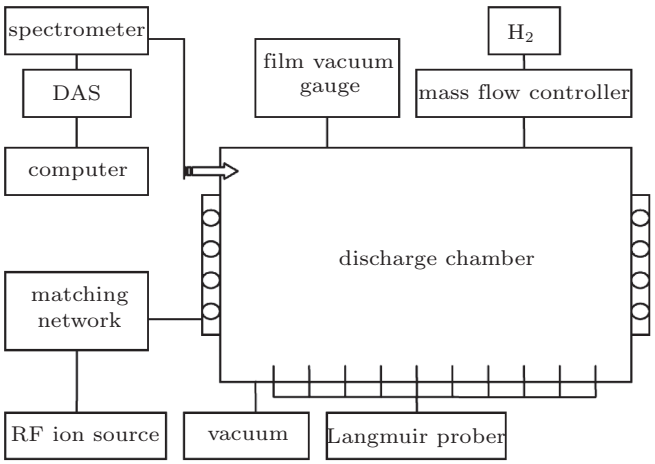

Fig. 1. Block diagram of the experimental setup.

was about 10^{-3} Pa. The working gas (H_2) was filled into the discharge chamber and kept at the constant pressure of 0.83 Pa during discharge.

The plasma diagnostic system consists of the optical emission spectrometer and 14 Langmuir probes. The resolution and appearance size of the spectrometer (andor-shamsock-SR-500i) are 0.05 nm and 550 mm×343 mm×206.5 mm, respectively. The precise calibration has been performed before leaving the factory. Diagnosis of Langmuir probes shows that the plasma density (N_e) is about 10^{17} m^{-3} and the plasma temperature T_e is about 5 eV.

3. Results and discussion

Under the discharge pressure of 0.83 Pa, the OES spectra at different RF powers are shown in Fig. 2. All the OES spectra are dominated by H_α and H_β emissions. Both H_α and H_β spectral line intensities obviously change with the RF power.

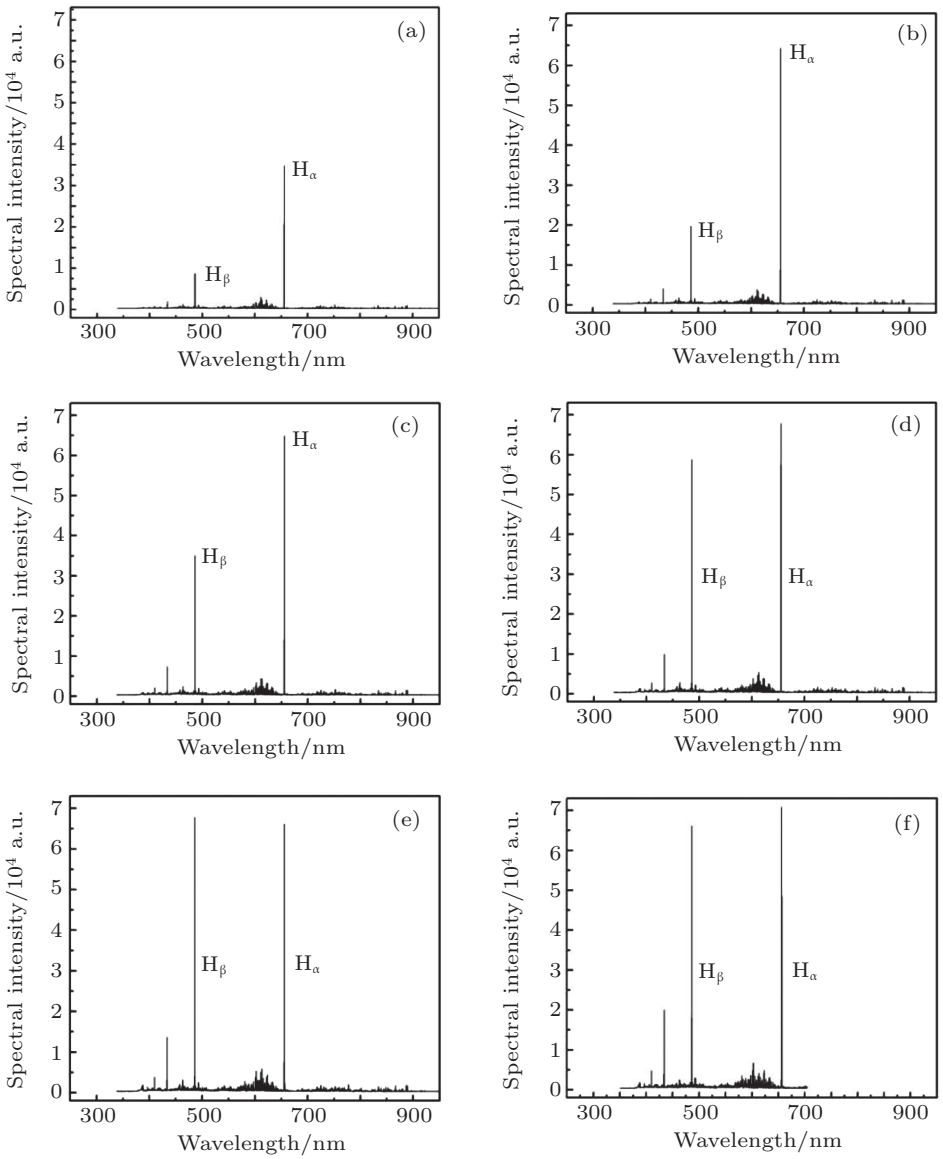

Fig. 2. OES spectra obtained at different RF powers: (a) 1 kW, (b) 2 kW, (c) 3 kW, (d) 4 kW, (e) 5 kW, and (f) 6 kW. a.u. denotes arbitrary units.

Figure 3 shows that the intensities of H_α ($\lambda = 656.28$ nm) and H_β ($\lambda = 486.13$ nm) spectral lines change with the wavelengths in hydrogen Balmer series, where Doppler broadening or Stark broadening is obvious in ICPs.[16,17]

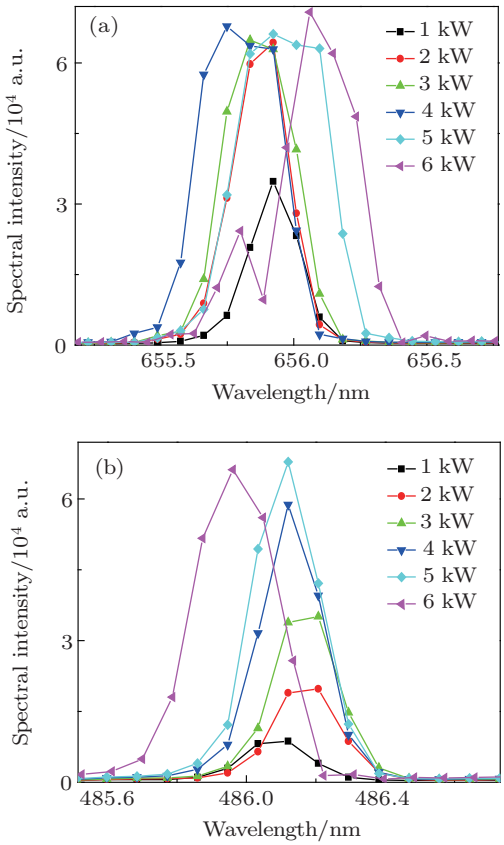

Fig. 3. (color online) H_α (a) and H_β (b) spectral line intensity with wavelength ranging from 1 to 6 kW. a.u. denotes arbitrary units.

As shown in Fig. 4, both I_α and I_β change with the input RF power. When the RF power is in the range of 0.0–2.0 kW, both I_α and I_β obviously increase with the RF power. However, when the RF power is in the range of 2.0–6.0 kW, I_α almost remains constant, but I_β obviously increases with the RF power.

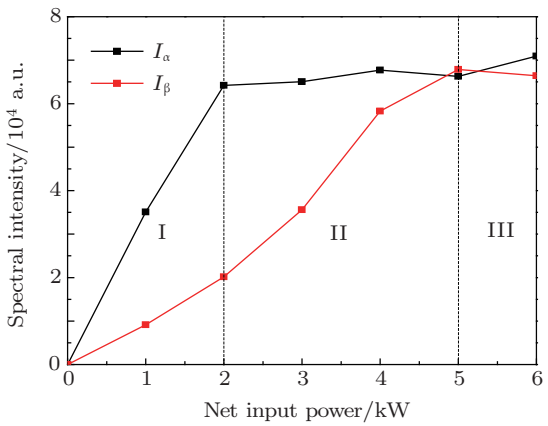

Fig. 4. (color online) Spectral intensities of H_α and H_β lines versus input RF power. a.u. denotes arbitrary units.

According to the hydrogen atom theory, H_α spectral line is emitted when the excited hydrogen atoms jump from E_3 to E_2 energy level, and the photon frequency is γ_{32}. Similarly, H_β spectral line is emitted when the excited hydrogen atoms jump from E_4 to E_2 energy level, and the photon frequency is γ_{42}, where $E_2 = -3.40$ eV, $E_3 = -1.51$ eV, and $E_4 = -0.85$ eV.[18]

For atom ray, the optical emission intensity I_{nm} of photon radiation (the transition for the excited states from the n-th to m-th energy level) at unit solid optical emission angle in light source can be expressed as follows:[16]

$$I_{nm} = \frac{h\gamma_{nm}}{4\pi} A_{nm} \frac{N_{\text{all}} g_n}{Z} \mathrm{e}^{-E_n/kT} = \frac{h\gamma_{nm}}{4\pi} A_{nm} N_n, \tag{1}$$

$$N_n = \frac{N_{\text{all}} g_n}{Z} \mathrm{e}^{-E_n/kT}, \tag{2}$$

where N_n is the number of hydrogen atoms in the n-th energy level, N_{all} the number of all hydrogen atoms, E_n the n-th energy level, Z the partition function, g_n the statistical weight in the n-th energy level, γ_{nm} the frequency of emitted photons, and A_{nm} is the transition probability.

As shown in Fig. 4, both I_α and I_β can be divided into three different RF power regions: region I (0.0–2.0 kW), region II (2.0–5.0 kW), and region III (5.0–6.0 kW).

3.1. Region I (0.0–2.0 kW)

In the low-pressure hydrogen plasma, the excited hydrogen atom is mainly produced by electron impact excitation. The main ways to produce the excited hydrogen atoms are the following dissociation excitation during the collision between fast electrons and the ground-state hydrogen molecules:

$$\mathrm{e(fast)} + \mathrm{H_2} \rightarrow \mathrm{H} + \mathrm{H}_{(n=3,4,5)}, \tag{3}$$

or the following direct excitation during the collision between fast electrons and the ground-state hydrogen atoms:[19,20]

$$\mathrm{e(fast)} + \mathrm{H} \rightarrow \mathrm{e} + \mathrm{H}_{(n=3)}, \tag{4}$$

where e(fast) is the fast electron, H_2 the ground-state hydrogen molecule, H the ground-state hydrogen atom, and $H_{(n)}$ the excited state hydrogen atom in the n-th energy level.

In order to analyze the hydrogen plasma spectrum, the corona model has to be used.[21,22] The excited state hydrogen atom density n_{H}^* in non-equilibrium plasmas can be expressed as

$$n_{\mathrm{H}}^* \sim n_{\mathrm{e}} n_{\mathrm{H}} X_{\mathrm{em,dir}} + n_{\mathrm{e}} n_{\mathrm{H_2}} X_{\mathrm{em,diss}}, \tag{5}$$

where n_{e} is the density of free electrons in hydrogen ICPs, n_{H} the density of ground-state hydrogen atoms, $X_{\mathrm{em,dir}}$ the hydrogen atom emission coefficient, n_{H2} the density of the ground-state hydrogen molecules, and $X_{\mathrm{em,diss}}$ the hydrogen molecular emission coefficient.

Although an increase in the electron temperature (1–2 eV) is very small in hydrogen ICPs, the electron density can rapidly increase with RF power.[20,23] According to the analytical results from Behringer *et al*,[22] both $X_{\mathrm{em,dir}}$ and

$X_{\mathrm{em,diss}}$ increase with the electron temperature, as shown in Fig. 5. According to Eq. (5), the density of excited hydrogen atoms significantly increases with the RF power if the density of both hydrogen atoms and molecules in the ground-state remains constant.

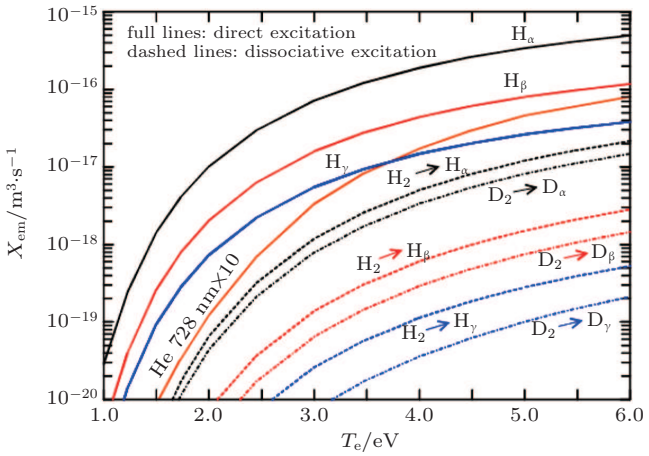

Fig. 5. (color online) Emission rate coefficients for three Balmer lines.[22]

Based on Eq. (1), for the special spectral line, both the spectral line frequency γ_{nm} and the transition probability A_{nm} are fixed. Since $h\gamma_{32} = E_3 - E_2 = 1.89$ eV and $h\gamma_{42} = E_4 - E_2 = 2.55$ eV, and for the transition coefficient τ_{nm} (the transition of excited states from the n-th to m-th energy level), $\tau_{32} = 44.10\ \mu_s^{-1}$ and $\tau_{42} = 8.419\ \mu_s^{-1}$,[24] we can obtain $\gamma_{32}A_{32} > \gamma_{42}A_{42}$. According to Boltzmann distribution law, we can obtain $N_3 > N_4$. Taking into account that H_α line is produced when the excited hydrogen atoms jump from E_3 to E_2 energy level, and H_β line is produced when the excited hydrogen atoms jump from E_4 to E_2 energy level, both I_α and I_β increase with the RF power, and $I_\alpha > I_\beta$. The theoretical explanation is well consistent with the experimental results obtained in the Region I (0.0–2.0 kW).

3.2. Region II (2.0–5.0 kW)

In region II, I_α does not increase with the RF power while I_β increases rapidly with the RF power. The theoretical explanation for the experimental results in region I is not applicable to that in region II.

Generally, it is difficult to produce the strong electric field in low-power RF plasmas although there is always a strong electric field at the sheath zone of the hydrogen plasmas.[25] However, it has been pointed out that the electric field intensity can be as high as 10^5 v·m^{-1} in the gas discharge tube.[16] We think that two kinds of strong electric fields can be produced in the hydrogen ICPs at an increasing RF power (> 2.0 kW): one is the strong external electric field produced from the high-power RF plasmas, and the other one is the strong internal micro electric field produced from the ions and electrons around the exited hydrogen atoms in the ICPs. Based on quantum mechanics, these strong electric fields can lead to a significant Stark effect, which plays a critical role in the changes of I_α and I_β in region II.

According to quantum mechanics, regardless of the electron spin and relativistic effects, the Hamiltonian operator $\hat{H}$ of hydrogen atoms in the external electric field ε is expressed as

$$\hat{H} = \hat{H}_0 + \hat{H}' = \hat{H}_0 + e\,\varepsilon\cdot\boldsymbol{r}, \quad \varepsilon = \varepsilon_1 + \varepsilon_2, \tag{6}$$

$$\hat{H}' = \hat{H}'_1 + \hat{H}'_2, \quad \hat{H}'_1 = e\,\varepsilon_1\cdot\boldsymbol{r}, \ \hat{H}'_2 = e\,\varepsilon_2\cdot\boldsymbol{r}. \tag{7}$$

In Eq. (6), $\hat{H}_0$ is the hydrogen atom Hamiltonian, ε_1 is the average value of the external induced electric field intensity, and ε_2 is the average value of the internal micro electric field intensity. In Eq. (7), $\hat{H}'_1$ is the electronic potential energy for the excited hydrogen atoms in the external induced electric field, and $\hat{H}'_2$ is the electronic potential energy for the excited hydrogen atoms in the internal micro electric field. The E_2, E_3, and E_4 are split into multiple energy levels, and the energy level in a hydrogen atom can be expressed as[26]

$$E_{nlm} = E_n^0 + E'_{nlm} = E_n^0 \pm \frac{3}{2}n(n-|m|-1)e\,\varepsilon\,a_0,$$
$$|m| = 0,\ 1,\ \ldots,\ n-1. \tag{8}$$

Equation (8) shows that the energy levels in the hydrogen ICPs only depend on the principal quantum number (n) and the magnetic quantum number (m). Thus, when the excited state hydrogen atoms jump from n_2 to n_1 energy level, the photon is emitted, and the photon frequency can be expressed as

$$\gamma_{n_2\to n_1} = \frac{E_{n_2}^0 - E_{n_1}^0}{h} + \frac{3e\varepsilon a_0}{2h}\left[\pm n_2(n_2-|m_2|-1) \pm n_1(n_1-|m_1|-1)\right],$$
$$|m_1| = 0,1,\ldots,n_1-1. \quad |m_2| = 0,1,\ldots,n_2-1. \tag{9}$$

According to the radiation transition selection rules: $\Delta m = 0, \pm 1$, as the hydrogen atom jumps from n_2 to n_1 energy level, the multiple number $N\ (n_2,\ n_1)$ for spectral lines can be described as

$$N(n_2,n_1) = (2n_2-1)(2n_1-1)\,. \tag{10}$$

Therefore, H_α line ($n_2 = 3 \to n_1 = 2$) is split into 15 spectral lines, while H_β line ($n_2 = 4 \to n_1 = 2$) is split into 21 spectral lines. Indeed, the latter can only be split into 15 spectral lines because of the same frequency.

As the RF power gradually increases, the density of excited hydrogen atoms can be greatly improved. Because $E_3 < E_4$, the hydrogen atoms can be easily excited to $n = 3$ splitting levels, then the hydrogen atoms in an excited state jump to $n = 2$ splitting levels, emitting H_α spectral lines. Taking into account that the number of excited hydrogen atoms must obey the Boltzmann distribution under a certain temperature, it

can be speculated that the number of hydrogen atoms in $n = 3$ splitting levels will firstly achieve its dynamic balance. Therefore, I_α almost remains constant in region II. However, owing to the Stark effect, $n = 4$ energy level is divided into seven splitting energy levels. Plenty of excited state hydrogen atoms achieve these energy levels, so a lot of excited hydrogen atoms in $n = 4$ splitting energy levels will jump to $n = 2$ splitting energy levels, emitting H_β line. This can explain why I_β rapidly increases with RF power in region II, and I_β achieves its maximum value so as to obey the Boltzmann distribution.

Owing to the strong Stark effect in the ICPs, the energy level could be split into three energy levels in $n = 2 : E_2 = E_{20}$, $E_{20} \pm 3e\varepsilon a_0$, in $n = 3 : E_3 = E_{30}$, $E_{30} \pm 4.5e\varepsilon a_0$, $E_{30} \pm 9e\varepsilon a_0$, and in $n = 4 : E_4 = E_{40}$, $E_{40} \pm 6e\varepsilon a_0$, $E_{40} \pm 12e\varepsilon a_0$, $E_{40} \pm 18e\varepsilon a_0$. For new exited energy levels, every energy level has the exited hydrogen atoms according to the Boltzmann distribution law. It is proved that the exited hydrogen atoms at lower energy levels are dominant when the system is in the thermal equilibrium, resulting in better distribution situation for more and more hydrogen atoms to achieve $n = 4$ energy levels. Then these excited state atoms jump from $n = 4$ to $n = 2$ energy levels, emitting H_β lines. As mentioned above, H_β spectral lines have been split into 15 spectral lines, which is helpful for improving the transition probability from $n = 4$ to $n = 2$ energy levels. Finally, taking into account Eq. (1), it can be concluded that I_β rapidly increases with the input RF power in region II.

3.3. Region III (5.0–6.0 kW)

In region III, both I_α and I_β reach their saturation states. With the further increase in the RF power, more fast electrons with high energy are produced, thus more excited hydrogen atoms with high energy will be produced in the plasma. Similarly, the excited hydrogen atoms under a certain temperature must obey the Boltzmann distribution. Therefore, on one hand, I_α stays in its saturation state, on the other hand, the number of hydrogen atoms at $n = 4$ splitting energy levels has to reach their dynamic balance, which explains why I_β remains its relative stable in the region III.

According to Fig. 4, when the RF power is close to 5.0 kW, I_α is ever bigger than I_β, which may be due to the experimental measurement deviation. However, it is noted that the gap between I_α and I_β is very small in the region III. We can see from Eq. (1) that, the light intensity depends mainly on three factors: the light transition frequency (γ_{nm}), the transition probability (A_{nm}), and the number of the excited hydrogen atoms (N_n). For H_α and H_β lines, the difference between γ_{32} and γ_{42} is obvious, and $\gamma_{32} < \gamma_{42}$. Based on Eq. (2), we have $N_3 > N_4$. However, N_3 is closer to N_4 when more and more hydrogen atoms in excited states jump to $n = 4$ energy levels and $n = 3$ energy levels have been at the saturation state. In addition, it is obvious to see that the ways for producing H_β spectral line are more than the ones for producing H_α spectral line. Therefore, the gap between A_{32} and A_{42} can be reduced. Thus, we obtain $\gamma_{32}A_{32}N_3 \sim \gamma_{42}\, A_{42}N_4$. According to Eq. (1), the gap between I_α and I_β could be very small in the region III.

4. Conclusion

In summary, we have obtained both the experimental results and the theoretical explanation on the spectral line intensities for H_α and H_β in Balmer lines in high-power (0.0–6.0 kW) hydrogen ICPs. In the region (0.0–2.0 kW), both I_α and I_β increase with the RF power, which is in good agreement with the experimental data published. However, in next region (2.0–6.0 kW), our experimental results deviate significantly from the theoretical explanation in the region (0.0–2.0 kW). Based on quantum mechanics, we think that with the increase in the electrical field, the Stark effect can play an important role in explaining the experimental results.

Acknowledgments

We would like to thank Li Ming, Bu Ying-Nan, Yu Li-Ming, Ni Wei-Yuan, and Liu Lu for providing us some measured results. We thank Prof. Lu Ming-Fang for beneficial discussion.

References

[1] Janev R K, Boley C D and Post D E 1989 *Nucl. Fusion* **29** 2125
[2] Hutchinson I H 2002 *Principles of Plasma Diagnostics* (Cambridge: Cambridge University Press)
[3] Fantz U 2004 *Plasma Phys.* **44** 508
[4] Duan X R, Lange H, Qian S J and Lang N 2003 *Chin. Phys. Lett.* **20** 489
[5] Cui J B and Fang R C 1996 *Chin. Phys. Lett.* **13** 192
[6] Johnson L C and Hinnov E J 1973 *Quantum Spectrosc. Radiat. Trans.* **13** 333
[7] Drawin H W and Emard F 1976 *Physica B* **85** 333
[8] Zikié R, Gignos M A, Ivković M, González M Á and Konjević N 2002 *Spectrochim Acta B* **57** 987
[9] Gignos M A, González M Á and Cardenoso V 2003 *Spectrochim Acta B* **58** 1489
[10] Chen C K, Wei T C, Collins L R and Phillips J 1999 *J. Phys. D: Appl. Phys.* **32** 688
[11] Satoru T, Xiao B J, Kazuki K and Morita M 2000 *Plasma Phys. Control. Fusion* **42** 1091
[12] Fantz U and Heger B 1998 *Plasma Phys. Control. Fusion* **40** 2023
[13] Zhu Y H, Wu W D, Tang Y J and Sun W G 2008 *Chin. J. Vac. Sci. Tech.* **28** 308 (in Chinese)
[14] Deng H Y, Wang J K, Wu W D, Cheng X L and Yang X D 2005 *J. At. Mol. Phys.* **4** 256 (in Chinese)
[15] Wang J K, Wu W D, Sun W G, Deng H Y, Cheng X L and Tang Y J 2005 *Chinese High Power Laser and Particle Beams* **10** 1513 (in Chinese)
[16] Qiu D R 2002 *Atomic Spectra Analysis* (1st edn.) (Shanghai: Fudan University Press) pp. 36–43 (in Chinese)

[17] Xin R X 2011 *Plasma Emission Spectra Analysis* (2nd edn.) (Beijing: Chemical Industry Press) p. 122 (in Chinese)
[18] Young H D and Freedman R A 2011 *Sears and Zemansky's University Physics with Modern Physics* (12th edn.) (Beijing: Mechanical Industry Press) p. 1317
[19] Keiji S and Takashi F 1995 *J. Appl. Phys.* **78** 2913
[20] Chen C K and Wei T C 1999 *J. Phys. D: Appl. Phys.* **32** 688
[21] Xiao B J, Kado S, Kajita S and Yamasaki D 2004 *Plasma Phys. Control. Fusion* **46** 653
[22] Behringer K and Fantz U 2000 *New J. Phys.* **2** 1
[23] Fang T Z, Wang L, Jiang D M and Zhang H X 2001 *Chin. Phys. Lett.* **18** 1098
[24] Tang P Y, Liu T, Ding B N and Dai J Y 2003 *Chinese High Power Laser and Particle Beams* **15** 293 (in Chinese)
[25] Mishra M K and Phukan A 2008 *Chin. Phys. Lett.* **25** 1011
[26] Zhang C X 2005 *Journal of Anhui Normal University (Natural Science)* **28** 407 (in Chinese)